Journal of Hazardous Materials 190 (2011) 36–44

Contents lists available at ScienceDirect

Journal of Hazardous Materials

journal homepage: www.elsevier.com/locate/jhazmat

Heavy metal ion adsorption behavior in nitrogen-doped magnetic carbon nanoparticles: Isotherms and kinetic study

Keun-Young Shin, Jin-Yong Hong, Jyongsik Jang*

School World Class University (WCU) Program of Chemical Convergence for Energy & Environment (C2E2), School of Chemical and Biological Engineering, College of Engineering, Seoul National University (SNU), Seoul, Republic of Korea

ARTICLE INFO

Article history:
Received 15 September 2010
Received in revised form 7 December 2010
Accepted 21 December 2010
Available online 25 December 2010

Keywords:
Polypyrrole
Nanoparticles
Carbonization
Heavy metal
Adsorption

ABSTRACT

To clarify the heavy metal adsorption mechanism of nitrogen-doped magnetic carbon nanoparticles (N-MCNPs), adsorption capacity was investigated from the adsorption isotherms, kinetics and thermodynamics points of view. The obtained results showed that the equilibrium adsorption behavior of Cr^{3+} ion onto the N-MCNPs can be applied to the Langmuir model and pseudo-second-order kinetics. It indicated that the fabricated N-MCNPs had the homogenous surface for adsorption and all adsorption sites had equal adsorption energies. Furthermore, the adsorption onto N-MCNPs taken place through a chemical process involving the valence forces. According to the thermodynamics, the adsorption process is spontaneous and endothermic in nature which means that the adsorption capacity increases with increasing temperature due to the enhanced mobility of adsorbate molecules. The effects of the solution pH and the species of heavy metal ion on the adsorption uptake were also studied. The synthesized N-MCNPs exhibited an enhanced adsorption capacity for the heavy metal ions due to the high surface area and large amount of nitrogen contents.

1. Introduction

The removal of heavy metal ions such as Cr^{3+}, Zn^{2+}, Ni^{2+}, Pb^{2+}, Ag^{+}, Hg^{2+} has attracted much attention due to their toxicity related to environmental problem all over the world. Especially, the Cr^{3+} ion has significantly harmful effect to ecological environment owing to the binding of the Cr^{3+} ion to proteins and nucleic acids [1,2].

Therefore, a large effort has been devoted to develop the ability to effectively remove heavy metal ions. The various approaches such as electrochemical method, ion exchange, membrane, solvent extraction and adsorption, have been suggested for remediation of heavy metal solution [3–7]. In particular, adsorption method can be considered as an effective and widely used process due to its simplicity and easy operational conditions. Up to date, several inorganic and organic adsorbents have been proposed for the adsorption method, including zeolites, clay minerals, trivalent and tetravalent metal phosphates, biosorbents and activated carbon [8–14]. Of a wide range of them, carbon-based materials have recently attracted a great deal of interest because of their inertness to surrounding environment, mechanical stability and highly porous structure with specific surface chemical properties [15–21]. However, they have shown limited efficiency as adsorbent for heavy metal uptake due to their irregular and micron-size of morphology. Furthermore, the additional process such as chemical oxidation, which incorporates both oxygen and nitrogen functional groups on the surface, should be involved for the enhanced adsorption capacity for heavy metal ion [22–27].

Recently, doping of heteroatom into carbon materials has attracted considerable attention for tailoring their chemical and physical properties [28,29]. From the point of view, we have previously reported on the fabrication of the nitrogen-doped magnetic carbon nanoparticles (N-MCNPs) [30–31] using the carbonization of multigram-scale polypyrrole nanoparticles (PPy NPs) as a carbon precursor [32–34]. This novel strategy does not require an additional process such as adding dopant material. Importantly, because the PPy NPs contain nitrogen atom which can endow two unpaired electrons, the synthesized N-MCNPs can be used as an adsorbent for adsorption of heavy metal ions.

Herein, we investigate the heavy metal ions uptake capacity of N-MCNPs according to the different solution pH, and then the Cr^{3+} ion uptake capacity as functions of contact time and adsorbate concentration is also described. Moreover, adsorption isotherms, kinetics and thermodynamics are also studied in order to understand the adsorption mechanism between the synthesized N-MCNPs and adsorbate. In advance, it is expected that the prepared monodispersed N-MCNPs have an enhanced heavy metal ion uptake and the magnetic property originated from the iron-

* Corresponding author. Fax: +82 2 888 1604.
E-mail address: jsjang@plaza.snu.ac.kr (J. Jang).

0304-3894/$ – see front matter.
doi:10.1016/j.jhazmat.2010.12.102

impregnated N-MCNPs makes it possible to efficiently separate and reuse the adsorbent under an external magnetic field.

2. Experimental

2.1. Materials

Pyrrole (98%), co-surfactant decyl alcohol (99%) and initiator ferric chloride ($FeCl_3$; 97%) were purchased from Aldrich Chemical Co. Heavy metals such as silver, chromium, lead, nickel, zinc and mercury were also prepared from their nitrate compounds of Aldrich Chemical Co and used without further purification. Surfactant dodecyltrimethylammonium bromide (DTAB) was supplied by TCI Co.

2.2. Fabrication of polypyrrole (PPy) nanoparticles

For the synthesis of the PPy nanoparticles with an average diameter of 60 nm, surfactant dodecyltrimethylammonium bromide (DTAB; 95.0 g, 308 mmol) was magnetically stirred in the mixture containing decyl alcohol (75.0 g, 474 mmol) and distilled water (2 L) at 3 °C. Subsequently, pyrrole (25 g, 372 mmol) was added dropwise to the surfactant solution and ferric iron chloride (140.2 g, 864 mmol) dissolved in a small amount of distilled water was introduced to the reaction mixture. The chemical polymerization of pyrrole monomer was conducted for 2 h at 3 °C. The resulting product was then transferred to a separating funnel and thoroughly washed with excess ethanol to remove the surfactant and other reagents. The upper solution containing surfactant and unreacted iron chloride was discarded and the precipitated nanoparticles were dried in a vacuum oven at room temperature. The amount of final product was very large as 24 g with a yield of 96%.

2.3. Fabrication of N-MCNPs

The iron-impregnated PPy nanoparticles were used as the carbon precursor to fabricate N-MCNPs. In a typical carbonization procedure, the PPy nanoparticles collected from the microemulsion polymerization were carried out in a quartz tubular furnace (21100 Tube furnace, Barnstead Thermolyne Corporation, USA) and precarbonized under nitrogen atmosphere. The sample was heated up to 800 °C at a heating rate of 3 °C min^{-1}, held for 3 h and then cooled to room temperature. Approximately 6 g of N-MCNPs could be obtained from 12 g of PPy precursor (a char yield of 50%).

2.4. Heavy metal extraction experiment

0.2 g of soluble chemical compounds containing different type of heavy metal ions (silver nitrate, chromium nitrate, lead nitrate, nickel nitrate, zinc nitrate, mercury nitrate) were added to 500 mL of distilled water containing 60% HNO_3 solution (19.2 mL), respectively. In order to control the pH, ammonia solution was injected into the heavy metal solution (50 mL). The adsorbent N-MCNPs (0.01 g) were introduced into the above solution and then shaken at 250 rpm for 12 h so that it would adsorb heavy metal ions. After the adsorption process, the solution was filtered through a 200 nm syringe filter and then the inductively coupled plasma (ICP) test was performed to analyze the concentration of heavy metal ions. For accurate adsorption results, the heavy metal adsorption was analyzed three times and the averaged value (error range: ±5%) was represented.

2.5. Effect of contact time on the adsorption process of heavy metal ion

The adsorption capacity for Cr^{3+} ion was monitored in 1 h step based on the pH 8 solution and initial concentration of Cr^{3+} ion (12.82 mg/L). The data for adsorption experiment to time were also measured three times by ICP test and the results were averaged. The standard deviation was less than 5%.

2.6. Recycling test for adsorption of heavy metal ion

The N-MCNPs in Cr^{3+} ion solution were separated by an external magnetic field (0.3 T) and then solvent was discarded. The residual N-MCNPs being loaded with Cr^{3+} ion were placed in 50 mL of distilled water containing 60% HNO_3 solution (1.92 mL) as a desorbing agent and then shaken at 250 rpm for 2 h. After that, the N-MCNPs in solution were separated again by a magnet, solvent was discarded again and the residual N-MCNPs were dried at 60 °C. Afterwards, the N-MCNPs were recycled for the adsorption of heavy metal ion by the same procedure described above. To determine the reusability of the N-MCNPs, consecutive recycling test were repeated five times using the same adsorbents.

2.7. Characterization

ICP measurement was performed by inductively coupled plasma-atomic emission spectrometer (ICPS-7500, SHIMADZU corporation, Japan). A field emission scanning electron microscopy (FE-SEM) images were obtained with a JEOL JSM-6700 F microscope. The XPS spectra were recorded using Kratos Model AXIS-HS system and the CHNS Elemental analysis was conducted with an EA1110 apparatus (CE instrument). The magnetic property of N-MCNPs was measured using a SQUID magnetometer (Quantum Design MPMS5).

3. Results and discussion

3.1. Fabrication of N-MCNPs

Fig. 1 represents the field emission scanning electron microscopy (FE-SEM) images of PPy NPs before and after the carbonization. The images exhibit that the PPy NPs and N-MCNPs had narrow size distribution and their average diameters were *ca.* 60 and 50 nm, respectively. Interestingly, the size of the N-MCNPs was smaller than that of the PPy NPs. Reduction in size can be explained by the aromatization and dehydrogenation of PPy NPs according to the carbonization [35].

To investigate nitrogen content of N-MCNPs, X-ray photoelectron spectroscopy (XPS) and elemental analysis were carried out. An XPS of the N-MCNPs is presented in Fig. 2. In the C 1s spectra, the main peak position of C 1s at 284.5 eV was attributed to aromatic C–C bonds and the second peak at 285.3 eV was related to C–N bonding. Furthermore, an N 1s spectrum definitely displayed the nitrogen species and was deconvoluted into pyridininc-N (398.5 eV) and pyrrolic-N (400.55 eV). Therefore, it was proved that nitrogen atoms of N-MCNPs were on aromatic C–C bond with pyridininc and pyrrolic form.

According to elemental analysis (Table 1), precursor PPy NPs consisted of C (49.0%), H (4.0%), N (13.4%) and S (0.0%). The C/N ratio of PPy NPs was *ca.* 3.7 since a repeating unit consists of four carbon atoms and a nitrogen atom, whereas in the N-MCNPs, C/N ratio was 7.0 owing to the carbonization process.

Judging from these data, it can be concluded that the monodispersed and multigram-scale N-MCNPs were successfully fabricated using the mild condition carbonization of PPy nanoparticles without the additional process. Moreover, N-MCNPs can be regarded as

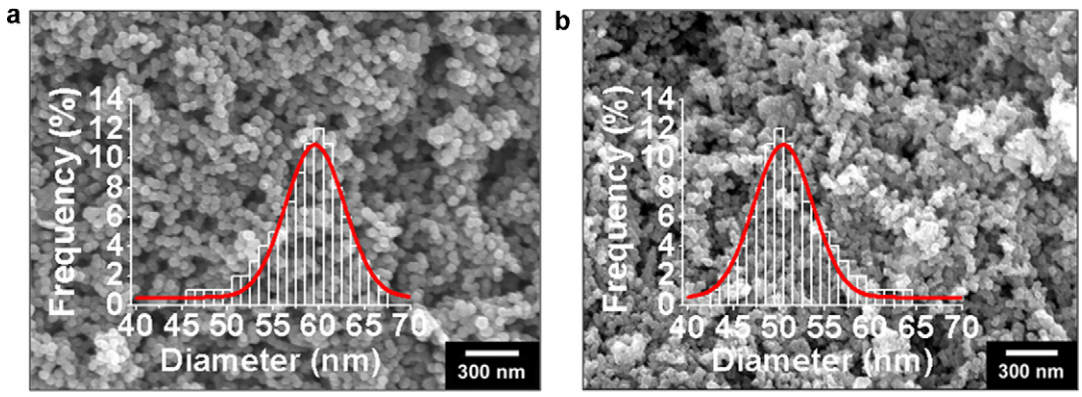

Fig. 1. FE-SEM images of (a) 60 nm PPy NPs synthesized by microemulsion method and (b) 50 nm N-MCNPs fabricated by using the carbonization of PPy NPs as a precursor (inset: Histograms of particle size distribution).

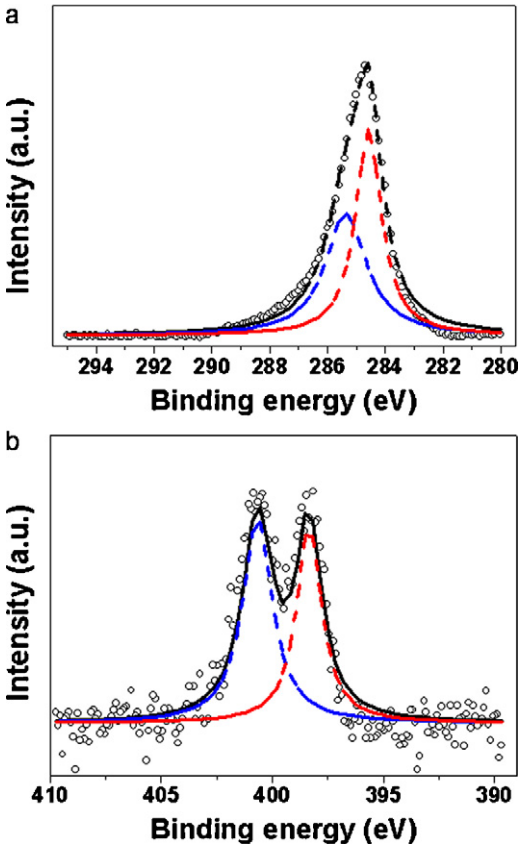

Fig. 2. (a) C 1s and (b) N 1s XPS spectra of N-MCNPs. Binding energy scale measured from Fermi level. In XPS spectra, blue, red lines of N 1s were ascribed to pyrrolic-N, pyridininc-N and blue, red lines of N 1s represented C–N bonds, aromatic C–C bonds, respectively. (For interpretation of the references to colour in this figure legend, the reader is referred to the web version of the article.)

Table 1
Elemental analysis of PPy NPs and N-MCNPs samples.

Sample	Atomic Ratio[a]			
	C (%)	H (%)	N (%)	S (%)
PPy NPs[b]	49.0	4.0	13.4	0.0
N-MCNPs[c]	63.0	1.0	9.0	0.0

[a] These values were obtained by elemental analyzer (EA1110, CE Instrument).
[b] The PPy NPs (avg. 60 nm) are washed five times with excess ethanol to remove impurities.
[c] The N-MCNPs are generally prepared by the carbonization of iron-impregnated PPy NPs precursor.

an excellent adsorbent for heavy metal ions due to the high contents of nitrogen with unpaired electrons which can combine with positively-charged heavy metal ions through chelation [36,37].

3.2. Effect of solution pH on the adsorption process of several heavy metal ions

In order to investigate the heavy metal ions removal capacity of N-MCNPs at pH values, several heavy metal ions such as chrome (Cr^{3+}), zinc (Zn^{2+}), nickel (Ni^{2+}), lead (Pb^{2+}), silver (Ag^{+}), mercury (Hg^{2+}) ions were selected as representative heavy metal ions. The heavy metal ion adsorption capacity was calculated by the following equation:

$$q_e = \frac{(c_o - c_e)V}{AW} \quad (1)$$

where q_e is the equilibrium adsorption capacity of adsorbent in mmol/g, C_o is the initial concentration of the heavy metal ions in mg/L, C_e is the equilibrium concentration of heavy metal ions after adsorption in mg/L, V is the volume of metal ions solution in L, and A is the atomic weight of heavy metal in g/mol, and W is the weight of the adsorbent in g. The adsorption equilibrium was gradually established within 12 h for all the tested metal ions. Accordingly, adsorption capacity of heavy metal ions solutions by N-MCNPs was measured after 12 h contact time.

Fig. 3 displays the effect of solution pH on the several heavy metal ions (Cr^{3+}, Zn^{2+}, Ni^{2+}, Pb^{2+}, Ag^{+}, Hg^{2+}) uptake onto the N-MCNPs. Interestingly, the N-MCNPs showed the high uptake capacity in the range of pH 6–10. This result can be ascribed to

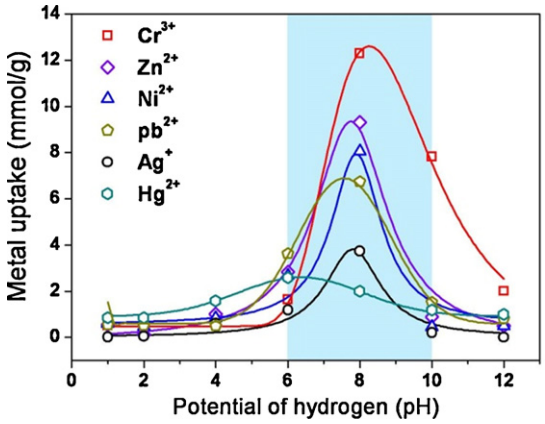

Fig. 3. Effect of solution pH on the several heavy metal ions (Cr^{3+}, Zn^{2+}, Ni^{2+}, Pb^{2+}, Ag^{+}, Hg^{2+}) uptake onto the N-MCNPs at 303 K (0.01 g adsorbent was added into 50 mL solution with 20 mg/L of adsorbate concentration).

the concentration of hydrogen (H^+) and hydroxyl (OH^-) ions compared to the heavy metal ion in the solution. Namely, in the low pH range, the concentration of heavy metal ions to bind unpaired electrons of adsorbent decreased with increasing the concentration of H^+ ions due to the acidification. In contrast, as the initial pH increased by injection of ammonia solution, the decrease of the H^+ ions concentration in the solution made it possible to increase the concentration of heavy metal ions to bind electrons, leading to a high adsorption uptake. However, when the basification was in progress (>pH 8), the precipitation attributed to the reaction between heavy metal ions and increased OH^- ions occurred and then the adsorption capacity has decreased. For this reason, the optimized pH was 8 for adsorption of heavy metal ions onto the N-MCNPs.

Under our experimental condition (pH 8), the amount of heavy metal ions uptake were *ca.* 12.28(Cr^{3+}), 9.31(Zn^{2+}), 8.06(Ni^{2+}), 6.74(Pb^{2+}), 3.73(Ag^+), 2.59(Hg^{2+}) mmol g^{-1}, respectively. Especially, the N-MCNPs had the selective preference for heavy metal ions such as chromium (Cr^{3+}), zinc (Zn^{2+}), nickel (Ni^{2+}) ions. This different adsorption efficiency can be explained as follows. In general, the functionalized materials exhibited unique selective affinity for binding heavy metal ions according to the type of soft or hard donor. Nitrogen has been regarded as a harder donor atom compared with sulfur, indicating that the N-MCNPs containing nitrogen atom exhibited higher complexation affinity for the harder metal ion (Cr^{3+}, Zn^{2+}, Ni^{2+}) than relatively softer metal ion (Pb^{2+}, Hg^{2+}) [38,39].

Notably, the maximum adsorption capacity of Cr^{3+} ion was *ca.* 10 times higher than that of naphthalenesulfonic acid on activated carbon (1.23 mmol g^{-1}) [40]. Moreover, N-MCNPs had enhanced Cr^{3+} ion adsorption over chitosan impregnated with microemulsion (2. 50 mmol g^{-1}) [41]. This improved adsorption capacity can be interpreted by the high surface area and large amount of nitrogen contents in the synthesized N-MCNPs.

3.3. Adsorption isotherms study

Fig. 4a and b show the experimental adsorption isotherms according to the initial and equilibrium Cr^{3+} ion concentration at room temperature. The obtained results showed that the removal of Cr^{3+} ion increased linearly with increasing the initial concentration, whereas with increasing equilibrium concentration, the uptake capacity rate decreased. To gain some insight into the adsorption process between the heavy metal ions and the N-MCNPs, the equilibrium adsorption data of heavy metal ions were fitted into the Langmuir [42], Freundlich [43] and D–R [44] isotherm equations.

Generally, the Langmuir adsorption isotherm describes the homogeneous surface assuming that the all the adsorption surface sites have identical adsorbate affinity and that adsorption at one site does not affect to an adjacent site. Furthermore, each adsorbate molecule has been located on a single site and hence it can be considered the monolayer formation of an adsorbate onto the adsorbent surface. The Langmuir equations are shown:

$$q_e = \frac{q_m b C_e}{1 + bC_e} \quad (\text{non linear form}) \quad \text{or} \quad \frac{C_e}{q_e} = \left(\frac{1}{q_m^b}\right) + \left(\frac{1}{q_m}\right) C_e \quad (\text{linear form}) \tag{2}$$

where q_m is the maximum amount of heavy metal uptake in mmol/g, b is the constant that refers to the bonding energy of adsorption related to free energy and net enthalpy in L/mg.

On the contrary, the Freundlich model describes the adsorption of a reversible heterogeneous surface since it does not restrict to the monolayer adsorption capacity.

The Freundlich isotherm is given as:

$$q_e = K_f C_e^{1/n} \quad (\text{non linear form}) \quad \text{or} \quad \log q_e = \log K_f + \frac{1}{n} \log C_e \quad (\text{linear form}) \tag{3}$$

where K_f is the constant related to the adsorption capacity of the adsorbent in mmol/g, and $1/n$ is the intensity of the adsorption constant. Despite the q_m and K_f were fundamentally differ, their values lead to the same conclusion related adsorption model. It is known that q_m is the monolayer adsorption capacity while K_f is the relative adsorption capacity. Nonlinear equation of regression analysis was carried out by OriginPro software (OriginPro 7.5, Originlab corporation, USA) in order to predict the parameters. The q_m, b, K_f, n values and the linear regression correlations for Langmuir (R^2), Freundlich (R^2) are listed in Table 2. The linear forms of the Langmuir and Freundlich equations are also shown in Fig. 4c and d.

Based on these data, it showed that the Langmuir isotherm fitted the data better with regression coefficients $R^2 = 0.9989$ and acceptable errors for parameters.

In particular, the Langmuir isotherm can be represented in terms of a dimensionless constant separation factor (R_L) [45,46]. The R_L is equal to the ratio of the unused adsorbent capacity to the maximum adsorbent capacity and thus it can be measurement of the adsorbent capacity used and the affinity between the adsorbate and adsorbent. R_L value was calculated by the following equation:

$$R_L = \frac{1}{1 + bC_o} \tag{4}$$

where b and C_o are the Langmuir constant and initial concentration of heavy metal ion. In general, R_L classified as $R_L > 1$, $R_L = 1$, $0 < R_L < 1$ and $R_L = 0$ indicates that the type of adsorption isotherm is unfavorable, linear, favorable and irreversible, respectively. Our R_L value was $0 < R_L < 1$ suggesting the favorable adsorption isotherm of Cr^{3+} onto the N-MCNPs (Fig. 4f).

Accordingly, it is considered that the fabricated N-MCNPs have the homogenous surface for adsorption and all sites have equal adsorption energies originated from the nitrogen atom of PPy nanoparticles.

Langmuir and Freundlich isotherms are insufficient to explain the chemical or physical properties of the adsorption process. However, the mean adsorption energy (E) calculated from the D–R isotherm can provide important information about these properties. The D–R isotherm, apart from being an analogue of the Langmuir isotherm, is more general because it does not assume a homogeneous surface or constant adsorption potential, and expressed as follows:

$$\ln q_e = \ln V_m' - K'\varepsilon^2 \tag{5}$$

where V_m' is the D–R adsorption capacity in mmol/g, K' is a constant related to the adsorption energy in mol^2/kJ^2, and ε is the Polanyi potential. ε is calculated with the following equation:

$$\varepsilon = RT \ln\left(1 + \frac{1}{C_e}\right) \tag{6}$$

where R is the gas constant (8.314×10^{-3} kJ/mol K) and T is the temperature (K).

The mean adsorption energy (E, kJ/mol) can be obtained from the K' value of the D–R isotherms using the following equation:

$$E = (-2K')^{-1/2} \tag{7}$$

For $E < 8$ kJ/mol, physisorption dominated the adsorption mechanism. If E is between 8 and 16 kJ/mol, the adsorption process

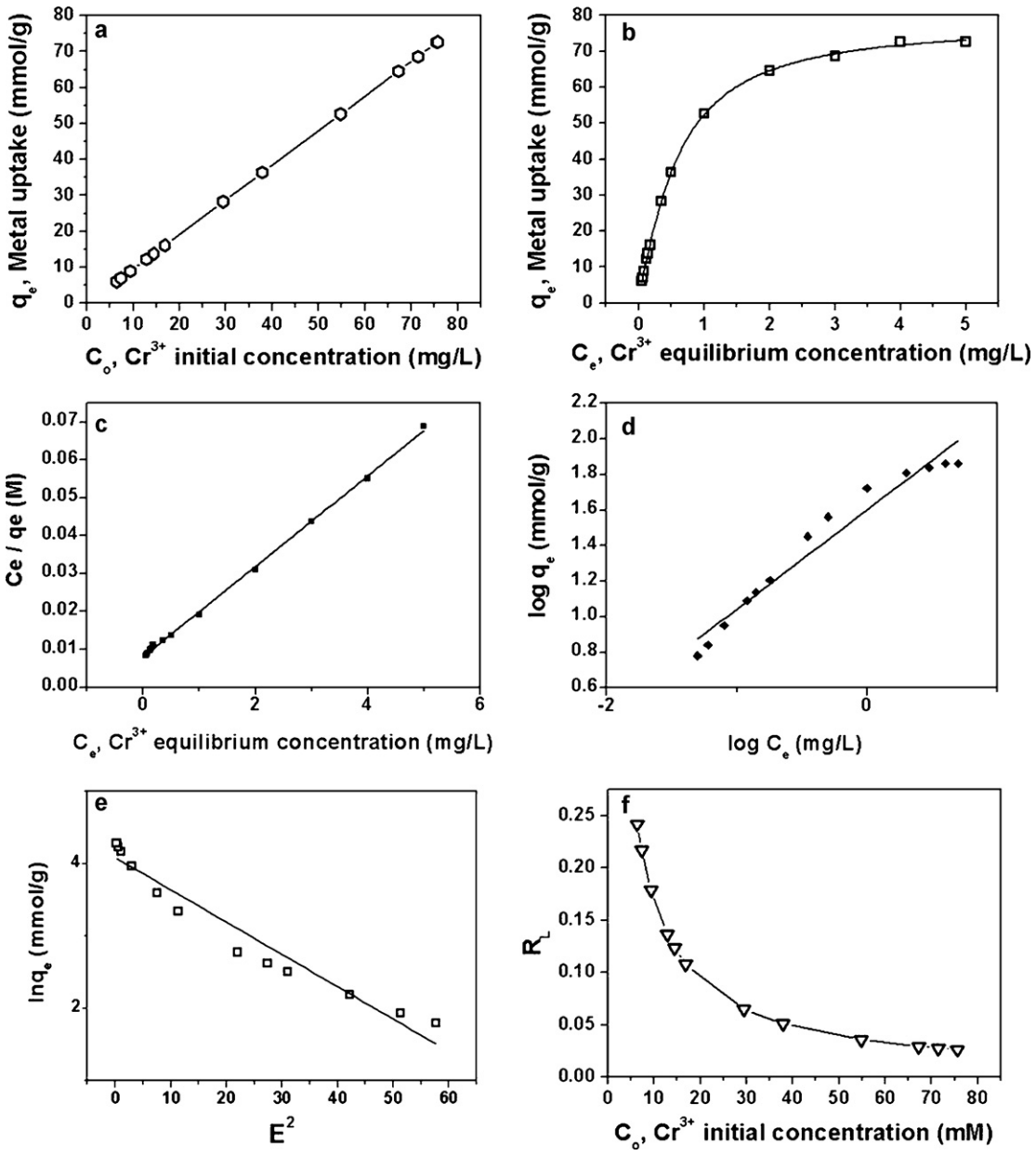

Fig. 4. Adsorption isotherm of Cr^{3+} ion onto N-MCNPs by (a) initial Cr^{3+} ion concentration (b) Cr^{3+} equilibrium ion concentration (c) Langmuir, (d) Freundlich (e) D–R isotherm equation (linear form). (f) Values of R_L for Langmuir equation.

follows chemical ion-exchange. The V'_m, K', E values and the linear regression correlations for D–R isotherm (R^2) are also listed in Table 2 and the linear forms of the equation is shown in Fig. 4e.

Based on these results, the calculated adsorption energy (10.5881 kJ/mol) indicated that adsorption mechanism of Cr^{3+} ion onto the N-MNCPs can be explained with an ion-exchange process.

3.4. Adsorption kinetic study

Cr^{3+} ion uptake of N-MCNPs was monitored as a function of contact time (Fig. 5a). The dotted line indicated that the adsorption capacity was saturated after 6 h. However, the reaction time was continued for 12 h to keep the sufficient condition for the stability of the adsorption equilibrium state.

Table 2
Adsorption parameters of the Langmuir, Freundlich and D–R isotherms at room temperature for the adsorption of Cr^{3+} ion on N-MCNPs.

Heavy metal ion	Langmuir			Freundlich			D–R isotherm			
	q_m (mmol/g)[b]	b (L/mg)[b]	$R^{2a,b}$	K_f (mmol/g)[b]	n[b]	$R^{2a,b}$	V'_m (mmol/g) [b]	K' (mol^2/kJ^2)[b]	E (kJ/mol)[b]	$R^{2a,b}$
Cr^{3+}	83.752 ± 0.0001	1.4925 ± 0.0002	0.9989	39.781 ± 0.0275	1.7922 ± 0.0351	0.9583	59.377 ± 0.0848	0.0045 ± 0.0003	10.588 ± 0.0031	0.9515

[a] R^2, regression coefficient.
[b] The q_m, b, K_f, n, V'_m, K', E values and the nonlinear regression correlations for Langmuir, Freundlich and D–R isotherms were measured by nonlinear regression analysis using OriginPro 7.5.

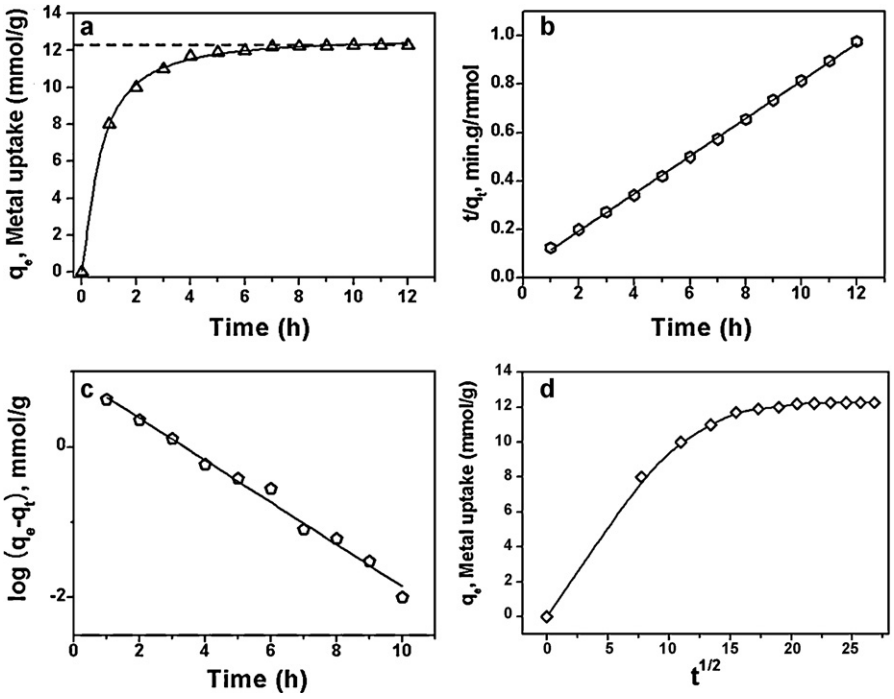

Fig. 5. Adsorption of Cr^{3+} ion onto N-MCNPs by (a) the contact time (b) pseudo-first-order kinetics, (c) pseudo-second-order kinetics and (d) intraparticle diffusion model.

To achieve an in-depth insight into the adsorption mechanism between Cr^{3+} ion and N-MCNPs, the pseudo-first-order [47,48], second-order kinetic [49–51], and intraparticle diffusion models [52] were fitted to the experimental data as shown in Fig. 5b–d.

In order to analyze the Cr^{3+} ion uptake rates to time, the pseudo-first-order equation was used as:

$$\log(q_e - q_t) = \log q_e - \frac{K_1}{2.303}t \quad (8)$$

where q_e and q_t are the heavy metal uptake at equilibrium and time t, respectively, and K_1 is the constant of first-order adsorption in min^{-1}. The pseudo-second-order equation is given as:

$$\frac{t}{q_t} = \frac{1}{K_2 q_e^2} + \frac{t}{q_e} \quad (9)$$

where, K_2 is the rate constant of second-order adsorption in $g\,mmol^{-1}\,min^{-1}$. For the detailed mechanism, intraparticle diffusion model is expressed with the equation given by Weber and Morris:

$$q_t = K_d t^{1/2} + C \quad (10)$$

where K_d is the intraparticle diffusion rate constant in $mmol\,g^{-1}\,min^{-0.5}$ and C is the thickness of the boundary layer.

Nonlinear equation of regression analysis was also carried out in order to predict the parameters. The q_{e1}, q_{e2}, K_1, K_2, K_d, C values were determined experimentally from the slope and intercept of straight-line adsorption kinetic plot. The values and regression coefficient are presented in Table 3.

Considering these data, it showed that the theoretical adsorption capacity values obtained from pseudo-second-order model were more consistent with regression coefficients $R^2 = 0.9995$ and acceptable errors for parameters. In general, the pseudo-second-order kinetic model assumes that the adsorption process occurs on localized sites with no interaction between adsorbates and maximum adsorption corresponds to a saturated monolayer of adsorbates onto the adsorbent surface. Furthermore, the rate of desorption is negligible compared to the rate of adsorption. For this reason, adsorption mechanism can be applied to the pseudo-second-order kinetics, leading to the chemical process due to the valence forces through sharing or exchange of electrons between the heavy metal ions and the N-MCNPs.

In addition, there are three main stages in the process of adsorption according to the intraparticle diffusion model (Fig. 5d). The Initial curved or steep-sloped portion represents the bulk diffusion or exterior adsorption rate which is very high. The subsequent linear portion is attributed to the intraparticle diffusion and the plateau portion is final equilibrium stage where the intraparticle diffusion starts to slow down due to extremely low solute concentrations in the solution. The regression coefficients of this line from the origin indicated that intraparticle diffusion was not the only operative mechanism and not the rate-determining step for the adsorption of Cr^{3+} ion onto the N-MCNPs.

Table 3
The kinetic adsorption parameters obtained using pseudo-first-order, pseudo-second-order and intraparticle diffusion models at room temperature for the adsorption of Cr^{3+} ion on N-MCNPs.

Heavy metal ion	Pseudo-first-order			Pseudo-second-order			Intraparticle diffusion		
	K_1 (min^{-1})	q_{e1} (mmol/g)	$R^{2a,b}$	K_2 (g/mmol min)[b]	q_{e2} (mmol/g)[b]	$R^{2a,b}$	K_d (mmol/gmin$^{0.5}$)[b]	C^b	$R^{2a,b}$
Cr^{3+}	0.645 ± 0.01072	8.81 ± 0.06652	0.9884	0.1558 ± 0.00382	12.89 ± 0.00052	0.9995	0.3764 ± 0.0680	4.0639 ± 1.2903	0.7357

[a] R_2, regression coefficient.
[b] The K_1, K_2, K_d, q_{e1}, q_{e2},C values and the nonlinear regression correlations for pseudo-first-order, pseudo-second-order and intraparticle diffusion models were measured by nonlinear regression analysis using OriginPro 7.5. The experimental value (q_e) was 12.28 mmol/g.

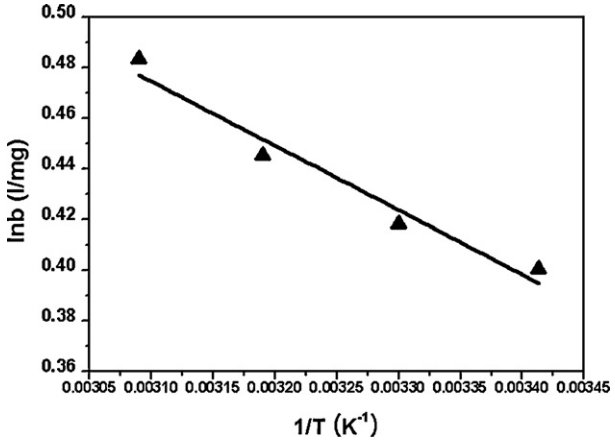

Fig. 6. Plot of the Langmuir isotherm constant at different temperature for the adsorption of Cr^{3+} ion onto N-MCNPs. The thermodynamic parameters in Table 4 are determined from this graph.

3.5. Adsorption thermodynamic study

The effect of temperature on Cr^{3+} ion adsorption of N-MCNPs is shown in Fig. 6. The experiments were carried out at 293, 303, 313 and 323 K. Thermodynamic parameters like free energy change (ΔG), enthalpy change (ΔH), and entropy change (ΔS) for the adsorption process were obtained using the following equations [53,54]:

$$\Delta G = RT \ln b \quad (11)$$

$$\Delta G = \Delta H - T\Delta S \quad (12)$$

$$\ln b = \left(\frac{\Delta s}{R}\right) - \left(\frac{\Delta H}{RT}\right) \quad (13)$$

The ΔH and ΔS values were determined experimentally from the slope and intercept of straight-line plot of $\ln b$ versus $1/T$. The values and regression coefficient are presented in Table 4.

The negative value for the ΔG indicates that the adsorption process is spontaneous and that the degree of spontaneity of the reaction increases with increasing temperature. The positive value of ΔH demonstrates that the adsorption process is endothermic in nature. It means that the adsorption capacity increases with increasing temperature due to the enhanced mobility of adsorbate molecules. The ΔS value was also positive. It can be originated from the redistribution of energy between the adsorbate and the adsorbent. Namely, before adsorption occurs, the heavy metal ions near the surface of the adsorbent will be more ordered, and the ratio of free heavy metal ions to interact with the adsorbent will be higher than in the subsequent adsorbed state. As a result, the distribution of rotational and translational energy among a small number of molecules increases with increasing adsorption. Therefore, the adsorption of Cr^{3+} ion onto the N-MCNPs occurred spontaneously at room and high temperatures.

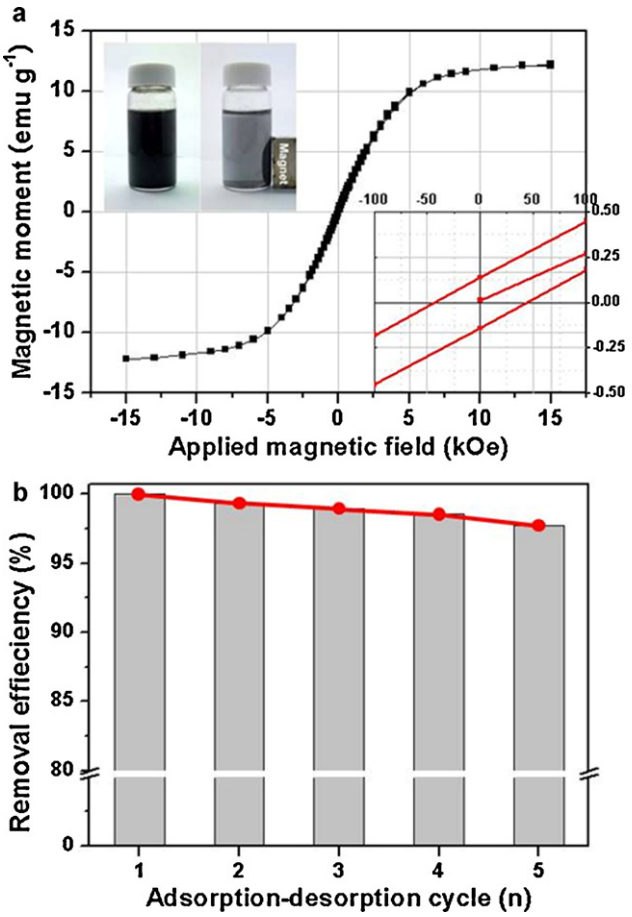

Fig. 7. (a) Magnetic property of N-doped MCNPs: Hysteresis loop (magnetization vs. applied field) of N-doped magnetic carbon nanoparticles at 300 K. The inset shows the hysteresis loop between −0.1 and 0.1 kOe. The photographs demonstrate that N-MCNPs can be attracted and arranged vertically by a magnet (0.3 T). (b) The recycling test for adsorption of Cr^{3+} ion onto the N-MCNPs.

3.6. Recycling test for adsorption of heavy metal ion

The magnetic properties of N-MCNPs were investigated using a SQUID magnetometer. In Fig. 6a, the hysteresis loop of N-MCNPs at 300 K shows the typical ferromagnetic characteristics (Fig. 7).

The magnetization could be measured with external magnetic fields ranging between ±15 kOe and the magnetization was saturated at 12.1 emu g^{-1}. In particular, the coercivity (H_C) from the expanded hysteresis loop between ±0.1 kOe was found to be 45.7 Oe. A significant enhancement of coercivity was observed in the N-MCNPs relative to the value for bulk iron ($H_C \approx 1$ Oe) because of the anisotropy of the magnetite embedded in the N-MCNPs. In addition, the digit photograph (Fig. 6b inset) demonstrates that the N-MCNPs in aqueous solution can be readily separated by an external magnetic field.

Table 4
Thermodynamic parameters for the adsorption of Cr^{3+} ion on N-MCNPs.

Heavy metal ion	T (K)	$\ln b$[b]	ΔG (kJ/mol)	ΔH (kJ/mol)[b]	ΔS (kJ/mol K)[b]	R^2[a,b]
Cr^{3+}	293	0.4005	−0.9755	2.1139 ± 0.2894	0.0105 ± 0.0009	0.9638
	303	0.4182	−1.0535			
	313	0.4453	−1.1589			
	323	0.4834	−1.2980			

[a] R_2, regression coefficient.
[b] The $\ln b$, ΔG, ΔH, ΔS values and the nonlinear regression correlations related to thermodynamic parameters were measured by nonlinear regression analysis using OriginPro 7.5.

From this point of view, N-MCNPs could provide the convenient reuse of adsorbent in solution by use of a magnetic field. Fig. 6b shows that there is almost no loss of removal efficiency (>97%) in recycling test and N-MCNPs could be reused up to 5 times for adsorption of Cr^{3+} ion. Therefore, it is expected that N-MCNPs could be a potential candidate as an excellent reusable and recoverable adsorbent of heavy metal ions [55].

4. Conclusions

The monodispersed and multigram-scale N-MCNPs were fabricated by carbonization of PPy nanoparticles as a carbon precursor. The synthesized N-MCNPs provided an enhanced and selective adsorption capacity for different heavy metal ions owing to the high surface area and high contents of nitrogen. Especially, the N-MCNPs had the 10-fold adsorption capacity for Cr^{3+} ion, compared to activated carbon with naphthalenesulfonic acid. Furthermore, they had the equal adsorption energies onto the homogenous surface for chemical adsorption process which is spontaneous and endothermic in nature and the iron-impregnated N-MCNPs were reused up to 5 times through the adsorption–desorption process.

Acknowledgement

This research was supported by a grant from the Center for Advanced Materials Processing (CAMP) of the 21st Century Frontier R&D Program funded by the Ministry of Knowledge Economy, WCU (World Class University) program through the National Research Foundation of Korea funded by the Ministry of Education, Science and Technology (R31-10013).

References

[1] J.O. Nriagu, J.M. Pacyna, Quantitative assessment of worldwide contamination of air, water and soils by trace metals, Nature 333 (1988) 134–139.
[2] Garcia-Reyes Refugio Bernardoa, Rangel-Mendez Jose Renea, Alfaro-De la Torre Ma. Catalinab, Chromium (III) uptake by agro-waste biosorbents: chemical characterization, sorption-desorption studies, and mechanism, J. Hazard. Mater. 170 (2009) 845–854.
[3] A.Y. Men'shikova, B.M. Shabsel's, T.G. Evseeva, Synthesis of polypyrrole nanoparticles by dispersion polymerization, Russ. J. Appl. Chem. 76 (2003) 822–826.
[4] A. Dabrowski, Z. Hubicki, P. Podkościelny, E. Robens, Selective removal of the heavy metal ions from waters and industrial wastewaters by ion-exchange method, Chemosphere 56 (2004) 91–106.
[5] Y. Takahashi, H. Kasai, H. Nakanishi, T.M. Suzuki, Test strips for heavy-metal ions fabricated from nanosized dye compounds, Angew. Chem. Int. Ed. 45 (2006) 913–916.
[6] S. Shin, J. Jang, Thiol containing polymer encapsulated magnetic nanoparticles as reusable and efficiently separable adsorbent for heavy metal ions, Chem. Commun. 41 (2007) 4230–4232.
[7] V.J.P. Vilar, C.M.S. Botelho, R.A.R. Boaventura, Influence of pH, ionic strength and temperature on lead biosorption by Gelidium and agar extraction algal waste, Process Biochem. 40 (2005) 3267–3275.
[8] U Wingenfelder, C. Hansen, G. Furrer, R. Schulin, Removal of heavy metals from mine waters by natural zeolites, Environ. Sci. Technol. 39 (2005) 4606–4613.
[9] A. Szabo, D. Gournis, M.A. Karakassides, D. Petridis, Clay–aminopropylsiloxane compositions, Chem. Mater. 10 (1998) 639–645.
[10] P. Sheng, Y.P. Ting, J.P. Chen, L. Hong, Sorption of lead, copper, cadmium, zinc, and nickel by marine algal biomass: characterization of biosorptive capacity and investigation of mechanisms, J Colloid Interface Sci. 275 (2004) 131–141.
[11] I. Ghorbel-Abid, A. Jrad, K. Nahdi, M. Trabelsi-Ayadi, Sorption of chromium (III) from aqueous solution using bentonitic clay, Desalination 246 (2009) 595–604.
[12] D. Mohana, C.U. Pittman Jr., Arsenic removal from water/wastewater using adsorbents – a critical review, J. Hazard. Mater. 142 (2007) 1–53.
[13] L. Khezami, R. Capart, Removal of chromium(VI) from aqueous solution by activated carbons: kinetic and equilibrium studies, J. Hazard. Mater. B123 (2005) 223–231.
[14] H. Tamai, T. Kakii, Y. Hirota, T. Kumamoto, H. Yasuda, Synthesis of extremely large mesoporous activated carbon and its unique adsorption for giant molecules, Chem. Mater. 8 (1996) 454–462.
[15] J. Bae, J. Jang, Carbon nanofiber/polypyrrole nanocable as toxic gas sensor, Sens. Actuators B 122 (2007) 7–13.
[16] K.J. Lee, S.H. Yoon, J. Jang, Carbon nanofibers: a novel nanofiller for nanofluid applications, Small 3 (2007) 1209–1213.
[17] M. Choi, J. Jang, Heavy metal ion adsorption onto polypyrrole-impregnated porous carbon, J. Colloid Interface Sci. 325 (2008) 287–289.
[18] Z. Li, M. Jaroniec, P. Papakonstantinou, J.M. Tobbin, U. Vohrer, S. Kumar, G. Attard, J.D. Holmes, Supercritical fluid growth of porous carbon nanocages, Chem. Mater. 19 (2007) 3349–3354.
[19] K. Ariga, A. Vinu, M. Miyahara, J.P. Hill, T. Mori, One-pot separation of tea components through selective adsorption on pore-engineered nanocarbon, carbon nanocage, J. Am. Chem. Soc. 129 (2007) 11022–11023.
[20] Y. Shin, G.E. Fryxell, W. Um, K. Parker, S.V. Mattigod, R. Skaggs, Sulfur-functionalized mesoporous carbon, Adv. Funct. Mater. 17 (2007) 2897–2901.
[21] C.M. Castilla, F.J. Maldonado-Hódar, Carbon aerogels for catalysis applications: an overview, Carbon 43 (2005) 455–465.
[22] S. Ko, J. Jang, Controlled amine functionalization on conducting polypyrrole nanotubes as effective transducers for volatile acetic acid, Biomacromolecules 8 (2007) 182–187.
[23] Y.L. Xing, M. Laurent, N.R. David, W. Heiko, H. Jurriaan, An in situ study of the adsorption behavior of functionalized particles on self-assembled monolayers via different chemical interactions, Langmuir 23 (2007) 9990–9999.
[24] M.E. Mahmoud, M.M. Osman, O.F. Hafez, E. Elmelegy, Removal and preconcentration of lead (II), copper (II), chromium (III) and iron (III) from wastewaters by surface developed alumina adsorbents with immobilized 1-nitroso-2-naphthol, J. Hazard. Mater. 173 (2010) 349–357.
[25] M Takafuji, S. Ide, H. Ihara, Z. Xu, Preparation of poly(1-vinylimidazole)-grafted magnetic nanoparticles and their application for removal of metal ions, Chem. Mater. 16 (2004) 1977–1983.
[26] C.A. Bell, S.V. Smith, M.R. Whittaker, A.K. Whittaker, L.R. Gahan, M.J. Monteiro, Surface-functionalized polymer nanoparticles for selective sequestering of heavy metals, Adv. Mater. 18 (2006) 582–586.
[27] B. Xiao, K.M. Thomas, Competitive adsorption of aqueous metal ions on an oxidized nanoporous activated carbon, Langmuir 20 (2004) 4566–4578.
[28] F.L. Deepak, N.S. John, A. Govindaraj, G.U. Kulkarni, C.N.R. Rao, Nature and electronic properties of Y-junctions in CNTs and N-doped CNTs obtained by the pyrolysis of organometallic precursors, Chem. Phys. Lett. 411 (2005) 468–473.
[29] Z. Yang, Y. Xia, R. Mokaya, Aligned N-doped carbon nanotube bundles prepared via CVD using zeolite substrates, Chem. Mater. 17 (2005) 4502–4508.
[30] H. Yoon, S. Ko, J. Jang, Nitrogen-doped magnetic carbon nanoparticles as catalyst supports for efficient recovery and recycling, Chem. Commun. 14 (2007) 1468–1470.
[31] B. Choi, H. Yoon, I.S. Park, J. Jang, Y.E. Sung, Highly dispersed Pt nanoparticles on nitrogen-doped magnetic carbon nanoparticles and their enhanced activity for methanol oxidation, Carbon 45 (2007) 2496–2501.
[32] H. Yoon, J. Jang, Formation mechanism of conducting polypyrrole nanotubes in reverse micelle systems, Langmuir 21 (2005) 11484–11489.
[33] H. Yoon, J. Jang, Multigram-scale fabrication of monodisperse conducting polymer and magnetic carbon nanoparticles, Small 1 (2005) 1195–1199.
[34] R. Ansari, N.K. Fahim, Application of polypyrrole coated on wood sawdust for removal of Cr(VI) ion from aqueous solutions, React. Funct. Polym. 67 (2007) 367–374.
[35] J.H. Oh, J. Jang, A facile synthesis of polypyrrole nanotubes using a template-mediated vapor deposition polymerization and the conversion to carbon nanotubes, Chem. Commun. 7 (2004) 882–883.
[36] A.K. Sengupta, Y. Zhu, D. Hauze, Metal(II) ion binding onto chelating exchangers with nitrogen donor atoms: some new observations and related implications, Environ. Sci. Technol. 25 (1991) 481–488.
[37] R.K. Dey, T. Patnaik, N. Mohapatra, Removal of heavy metal ions using new chelating material containing N, O, and S donor sites, Sep. Sci. Technol. 42 (2007) 3593–3608.
[38] A.M Liu, K. Hidajat, S. Kawi, D.Y. Zhaob, A new class of hybrid mesoporous materials with functionalized organic monolayers for selective adsorption of heavy metal ions, Chem. Commun. 13 (2000) 1145–1146.
[39] V. Antochshuk, O. Olkhovyk, M. Jaroniec, I.S. Park, R. Ryoo, Benzoylthiourea-modified mesoporous silica for mercury(II) removal, Langmuir 19 (2003) 3031–3034.
[40] M. Sánchez-Polo, F. Carrasco-Marín, J. Rivera-Utrilla, Adsorption of 1,36-naphthalenetrisulfonic acid on activated carbon in the presence of Cd(II), Cr(III), and Hg(II). Importance of electrostatic interactions, Langmuir 19 (2003) 10857–10861.
[41] A.A. Dantas Neto, M.C.P. de, A. Moura, E.L. Barros Neto, E. de Paiva Telemaco, T.N. de Castro Dantas, Chromium adsorption by chitosan impregnated with microemulsion, Langmuir 17 (2001) 4256–4260.
[42] I. Langmuir, The adsorption of gases on plane surfaces of glass, mica and platinum, J. Am. Chem. Soc. 40 (1918) 1361–1403.
[43] H. Freundlich, W.J. Helle, The adsorption of cis- and trans-azobenzene, J. Am. Chem. Soc. 61 (1939) 2228–2230.
[44] N. Unlu, M. Ersoz, Adsorption characteristics of heavy metal ions onto a low cost biopolymeric sorbent from aqueous solutions, J. Hazard. Mater. B136 (2006) 272–280.
[45] A. Corami, S. Mignardi, V.J. Ferrini, Copper and zinc decontamination from single- and binary-metal solutions using hydroxyapatite, J. Hazard. Mater. 146 (2007) 164–170.
[46] M. Rafatullaha, O. Sulaimana, R. Hashima, A. Ahmadb, Adsorption of copper (II), chromium (III), nickel (II) and lead (II) ions from aqueous solutions by meranti sawdust, J. Hazard. Mater. 170 (2009) 969–977.
[47] Y.S Ho, D.A.J. Wase, C.F. Foster, Kinetic studies of competitive heavy metal adsorption by sphagnum moss peat, Environ. Technol. 17 (1996) 71–77.

[48] S. Lagergren, Zur theorie der sogenannten adsorption geloster stoffe, K. Sven Vetenskapsakad Hanndl. 24 (1898) 1–39.
[49] G. McKay, M.J. Bino, A.R. Altamemi, The adsorption of various pollutants from aqueous solutions on to activated carbon, Water Res. 19 (1985) 491–495.
[50] M.S. Bilgili, Adsorption of 4-chlorophenol from aqueous solutions by xad-4 resin: isotherm, kinetic, and thermodynamic analysis, J. Hazard. Mater. 137 (2006) 157–164.
[51] D. Mohan, C.U. Pittman Jr., M. Bricka, F. Smith, B. Yancey, J. Mohammad, P.H. Steele, M.F. Alexandre-Franco, V. Gómez-Serrano, H. Gong, Sorption of arsenic, cadmium, and lead by chars produced from fast pyrolysis of wood and bark during bio-oil production, J. Colloid Interface Sci. 310 (2007) 57–73.
[52] W.J Weber, J.C. Morris, Kinetics of adsorption on carbon from solutions, J. Sanit. Engng. Div. Am. Soc. Civ. Eng. 89 (1963) 31–60.
[53] M.S. Mohy-Eldin, M.F. Elkady, M.A. Abu-Saied, A.M. Abdel Rahman, E.A. Soliman, A.A. Elzatahry, M.E. Youssef, Removal of cadmium ions from synthetic aqueous solutions with a novel nanosulfonated poly(glycidyl methacrylate) cation exchanger: kinetic and equilibrium studies, J. Appl. Polym. Sci. 118 (2010) 3111–3122.
[54] M.E. Argun, S. Dursun, C. Ozdemir, M. Karatas, Heavy metal adsorption by modified oak sawdust: thermodynamics and kinetics, J. Hazard. Mater. 141 (2007) 77–85.
[55] Q. Hu, Z. Fang, X. Zhang, B. Zhang, X. Liu, Magnetic chitosan nanocomposites: a useful recyclable tool for heavy metal ion removal, Langmuir 25 (2009) 3–8.